


Jamming densities of random sequential adsorption on d -dimensional cubic latticesAsher Baram and Azi Lipshtat *Soreq Nuclear Research Center, Yavne 81800, Israel*

(Received 7 January 2021; revised 27 April 2021; accepted 4 June 2021; published 6 July 2021)

The rate of convergence of the jamming densities to their asymptotic high-dimensional tree approximation is studied, for two types of random sequential adsorption (RSA) processes on a d -dimensional cubic lattice. The first RSA process has an exclusion shell around a particle of nearest neighbors in all d dimensions ($N1$ model). In the second process the exclusion shell consists of a d -dimensional hypercube with length $k = 2$ around a particle ($N2$ model). For the $N1$ model the deviation of the jamming density $\rho_r(d)$ from its asymptotic high d value $\rho_{\text{asy}}(d) = \frac{\ln(1+2d)}{2d}$ vanishes as $[\frac{\ln(1+2d)}{2d}]^{3.41}$. In addition, it has been shown that the coefficients $a_n(d)$ of the short-time expansion of the occupation density of this model (at least up to $n = 6$) are given for all d by a finite correction sum of order $(n - 2)$ in $1/d$ to their asymptotic high d limit. The convergence rate of the jamming densities of the $N2$ model to their high d limits $\rho_{\text{asy}}(d) = d^{\frac{\ln 3}{3d}}$ is slow. For $2 \leq d \leq 4$ the generalized Palasti approximation provides by far a better approximation. For higher d values the jamming densities converge monotonically to the above asymptotic limits, and their decay with d is clearly faster than the decay as $(0.432\ 332 \dots)^d$ predicted by the generalized Palasti approximation.

DOI: [10.1103/PhysRevE.104.014104](https://doi.org/10.1103/PhysRevE.104.014104)**I. INTRODUCTION**

Random sequential adsorption (RSA) is an irreversible random filling process [1,2]. In this process nonoverlapping particles are randomly adsorbed sequentially into a d -dimensional space. The filling process is subject to constraints imposed by interactions with previously deposited particles. For particles interacting via short-range hard-core repulsion, an exclusion shell, that depends on the geometry of the interaction, is formed around each adsorbed particle. The adsorbed particles and their exclusion shells are immobile, thus their positions are fixed for the entire RSA process. At each step in the deposition process a new particle is either rejected without affecting the population of the already occupied sites, or the new particle is added at random at an accessible site in the volume. As a result, the density of adsorbed particles increases monotonically with time. Since the particles and their exclusion shells are formed randomly, and their positions are fixed for the entire process, noncompact configurations are formed. Therefore the process ceases in a nonequilibrium jammed state, whose average occupation density $\rho(t = \infty) = \rho_r$ —jamming density—is smaller than the corresponding density of closest packing.

In 1939 Flory [3] considered the dynamics of a cyclization reaction among neighboring side groups along a polymer chain. He found that the kinetic of this chemical process is mathematically equivalent to a RSA filling of dimers on a one-dimensional (1D) lattice, and obtained an analytic expression for the entire process including its jamming density. Renyi solved the continuum analog, i.e., the random deposition of unit line segments on a one-dimensional continuum, known as the car parking model [4]. RSA models are realized by many physical, chemical, biological compaction, and eco-

logical processes in various spatial dimensionalities [1,2,5–8]. All these processes are characterized by a slow diffusion rate compared to the timescale of the deposition, resulting in a nonequilibrium state. Since the RSA phase is a disordered state for all values of the occupation density $\rho(t)$, it has been suggested as a phenomenological model for glasses and supercooled liquids [9–12]. The RSA process is investigated on continuous, discrete, and fractal lattices [13,14]. A high-dimensional packing density has been shown to relate to digital communication protocols [15] and to the phase behavior of glassy states of matter [16,17].

Exact solutions for RSA models are available for only a few limiting cases: lattice and continuum 1D systems [3,4,18,19], a quasi-1D two-row model (ladder model) [20–22], and the infinite dimensionality limit [23,24]. In addition, the asymptotic approach of the density to its jamming limit is known to be given by an algebraic time dependence for continuum systems [25,26] and by an exponential time dependence for lattice models [2,27].

The information for the RSA dynamics of general systems stems from numerical Monte Carlo (MC) computations [28–33], and from formal short-time series expansions [23,27,34–37]. The series expansion method is similar in principle to the Mayer cluster expansion for equilibrium systems. Indeed, the first two coefficients of the RSA density series in terms of time t are identical to the two first coefficients of the cluster expansion [34]. A deviation of RSA systems from the equilibrium value starts at the third term of their expansion. For lattice models the computation of the coefficients is equivalent to a counting problem that can be automated [27,36], and the available coefficients usually suffice to provide quite accurate approximations for the jamming densities.

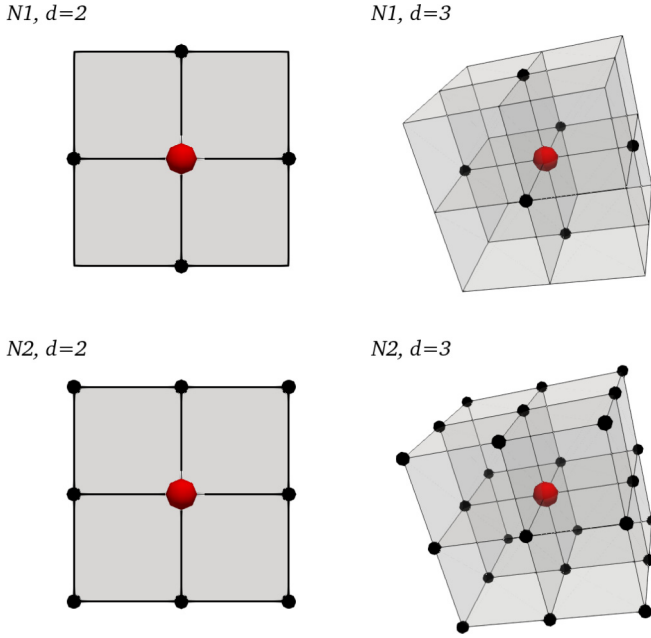


FIG. 1. The interacting sites in the two models for $d = 2, 3$. The adsorbed particle is marked by the large red sphere, and the sites it interacts with are marked by black small spheres.

In this paper we study the convergence of the jamming densities to their asymptotic high d values as a function of the spatial dimensionality d . We study the RSA on the d hypercubic lattice for two types of exclusion interactions: (1) nearest-neighbor exclusion ($N1$ model), and (2) exclusion of d -dimensional cubes with length $k = 2$ around the particle ($N2$ model).

In the $N1$ model a particle interacts with nearest-neighbor deposition sites along one of the d axes. There are two neighbors on each direction, one from each side of the particle, and thus each particle interacts with $q = 2d$ sites. In the $N2$ model the repulsion interaction is extended to the d -dimensional hypercube with an edge length of 2 around the particle. This hypercube includes all of the grid points whose coordinates differ in not more than 1 from the particle coordinates, i.e., diagonal neighbors are also considered in the exclusion shell. Since any of the d coordinates may be equal to the respective coordinate of the particle, larger in 1 or smaller in 1, there are in total $q = 3^d - 1$ interacting sites around the particle (Fig. 1).

II. GENERAL THEORY

The occupation density of the adsorbed particles in the RSA process is given by a diagrammatic expansion in the short-time variable $1 - u$, where $u = e^{-t}$ [23],

$$\rho(t) = \sum_{n=1}^{\infty} \frac{(-1)^{n-1} a_n (1-u)^n}{n!}. \quad (1)$$

The coefficient a_n is a positive integer, that equals the number of connected lattice animals that may be formed at the n th time step. Each of these lattice animals contains n points, and the connectivity range among the points is determined by the

range of the interparticle interaction. In the $N1$ model points can be connected if there is a difference of 1 in one (and only one) of their coordinates. In the $N2$ model any number of coordinates may differ by 1 to allow connectivity. For all models, $a_1 = 1$.

At the second step the number of the lattice points connected to the starting point, a_2 , depends on the interparticle interaction and the type of the lattice. For the $N1$ model $a_2 = q = 2d$ the number of nearest neighbors of the starting point. For the $N2$ model $a_2 = 3^d - 1$ the number of lattice points (excluding the starting point) contained in a d -dimensional hypercube.

At the third step a three-point connected lattice animal is formed by adding a point to one of the empty neighbors of each of the two point animals. The number of empty neighbors is called the perimeter of an animal. The growth rate of the coefficients a_{n+1}/a_n is determined by the average perimeter of the n th lattice animal. The computation of the a_n coefficients reduces to an enumeration problem on a lattice, and algorithms for the computation are presented in Refs. [27,36].

It is worthwhile to mention that an equivalent expansion for $\rho(t)$ in terms of powers of t is given by

$$\rho(t) = \sum_{n=1}^{\infty} \frac{(-1)^{n-1} b_n t^n}{n!}. \quad (2)$$

The relation between the two sets of coefficients is given by

$$b_n = \sum_{m=1}^n S_{n,m} a_m, \quad (3)$$

where $S_{n,m}$ is a Stirling number of the second kind [38]. It is easy to see that b_n is a positive integer substantially larger than a_n .

Baram and Kutasov [23] observed that for large spatial dimensionality d most of the points of a lattice animal have $(q - 1)$ empty neighbors. The probability to curl and form a compact animal is negligible. Thus most of the animals are acyclic graphs (trees). Since $q \approx (q - 1)$, the coefficients are related by the recursion relation,

$$a_n = (n - 1)q a_{n-1} \quad (4)$$

or

$$a_n = (n - 1)! a_2^{n-1} \quad (5)$$

By substituting Eq. (5) into Eq. (1), one obtains for the asymptotic (large d) density

$$\rho_{\text{asy}}(t) = \frac{\ln[1 + (1 - u)a_2]}{a_2}. \quad (6)$$

For this approximation, the limit value at $t \rightarrow \infty$ (i.e., $u \rightarrow 0$) for the density is

$$\rho_{\text{asy}} = \frac{\ln[1 + a_2]}{a_2}. \quad (7)$$

Fan and Percus [24], using similar arguments for $N1$ -type models, found the following asymptotic expression,

$$\begin{aligned} \rho_{\text{FP}} &= \frac{1}{2} [1 - (q - 1)^{-2/(q-2)}] \\ &= \frac{\ln(q - 1)}{q - 2} - \left[\frac{\ln(q - 1)}{q - 2} \right]^2 + O(1/q^3). \end{aligned} \quad (8)$$

TABLE I. MC estimations for the jamming densities as a function of dimensionality d . L is the length of the lattice, and N_{sim} number of simulations for this combination of d and L .

d	L	L^d	N_{sim}	ρ	std
2	100	10000	2000	0.364 122	2.4×10^{-3}
2	400	160 000	1000	0.364 124	6.0×10^{-4}
3	50	125 000	100	0.305 473	8.8×10^{-4}
3	100	1000 000	100	0.305 402	2.8×10^{-4}
4	50	6250 000	290	0.263 875	1.2×10^{-4}
5	12	248 832	2000	0.233 192	6.2×10^{-4}
5	24	7962 624	90	0.233 180	1.0×10^{-5}
6	10	1000 000	877	0.209 579	3.0×10^{-4}
6	12	2985 984	50	0.209 600	1.5×10^{-4}
7	8	2097 152	600	0.190 787	1.9×10^{-4}
8	8	16 777 216	40	0.175 424	6.5×10^{-5}

Given that $a_2 = q$, at the high d limit both Eqs. (7) and (8) converge to the same value, which is given by the leading term of Eq. (8) and decays as $1/q$.

III. RSA JAMMING DENSITIES OF THE $N1$ MODEL ON HYPERCUBIC LATTICES

The coordination number of a particle interacting via a hard-core interaction with its nearest neighbors ($N1$ model) on the d -dimensional hypercubic lattice is $2d$. Thus the tree approximation [23] predicts that the asymptotic jamming density is given by

$$\rho_{\text{asy}}(d) = \ln(1 + 2d)/2d. \tag{9}$$

In order to determine the rate of convergence to the asymptotic limit as a function of d , we compute by both MC simulations and by summations of the short-time expansions [Eq. (1)] accurate estimations for the jamming densities $\rho_r(d)$, for $2 \leq d \leq 8$. The MC simulations are performed on a d -dimensional hypercubic lattice with L^d sites with periodic boundary conditions in all directions. The RSA filling process starts with an empty lattice. At each step one vacant site is randomly selected. This site and its exclusion shell neighbors are marked as occupied. The process ceases when there are no available vacant sites. The jamming density is the ratio

between the number of particles required for filling the lattice (i.e., number of steps in the simulation) and total number of sites. Due to computation limitations, the lattice size and number N_{sim} of simulations decrease with the number of sites, as indicated by Table I.

It should be noted that despite the size limitation, there are no finite-size effects in our results. In Fig. 2 we present the results of the MC simulations for several lattice sizes. It is shown that $L = 6$ is sufficient to provide a good estimation of the jamming density, and considering a larger lattice does not considerably change this estimation.

The perimeter of a two-point lattice animal equals $2(2d - 1)$. As a result, the third coefficient $a_3(d)$ is given by

$$a_3(d) = 2 \times (2d)^2 [1 - 1/2d]. \tag{10}$$

The coefficient deviates from its large- d asymptotic value [Eq. (5)] by a factor of $(1 - 1/2d)$. For higher $n = 4-7$ we enumerated the connected lattice animals for all $d < 9$, and obtained all the coefficients $a_n(d)$. Note that for $d = 1$, $a_n(1) = 2^{n-1}$ for all n . For $d = 2$ the coefficients $a_n(2)$ are already known up to $n = 18$ [27]. The available $a_n(d)$'s are consistent with the following correction finite series to their asymptotic high d expression,

$$a_n(d) = (n - 1)! (2d)^{n-1} \left[1 - \sum_{j=1}^{n-2} (-1)^{j-1} f_{n,j} / d^j \right], \tag{11}$$

where $f_{n,j}$ are positive rational numbers for all n and j .

In particular,

$$a_4(d) = 6 \times (2d)^3 [1 - 4/(3d) + 1/(2d^2)], \tag{12}$$

$$a_5(d) = 24 \times (2d)^4 [1 - 19/(8d) + 49/(24d^2) - 5/(8d^3)], \tag{13}$$

$$a_6(d) = 120 \times (2d)^5 [1 - 427/(120d) + 151/(30d^2) - 793/(240d^3) + 67/(80d^4)]. \tag{14}$$

Consistency with the 1D coefficients requires that

$$1 - \sum_{j=1}^{n-2} (-1)^{j-1} f_{n,j} = 1/(n - 1)!$$

for all n .

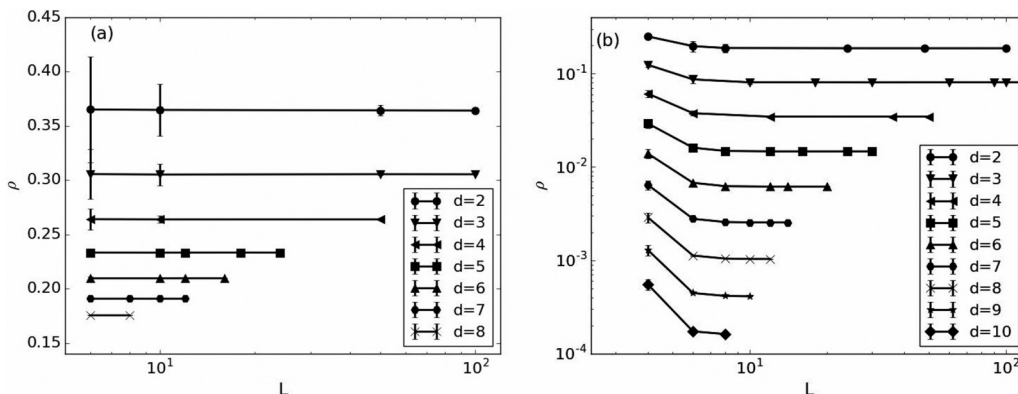


FIG. 2. Lattice size dependence of the jamming density for (a) $N1$ model and (b) $N2$ model. Note that for better presentation the y axis of (a) is in linear scale whereas (b) is presented in logarithmic scale.

TABLE II. Estimations for the jamming densities vs dimensionality d . Top to bottom: Asymptotic values [computed using the asymptotic expression presented at Eq. (9)], MC estimations, Levin summation of six coefficients, and Fan and Percus high d approximation [Eq. (8)].

d	2	3	4	5	6	7	8
ρ_{asy}	0.402 36	0.324 32	0.274 65	0.239 79	0.213 74	0.193 43	0.177 07
MC	0.364 12	0.3054	0.263 87	0.2332	0.209 58	0.190 79	0.175 42
Levin	0.364 06	0.3056	0.264 12	0.2333	0.209 70	0.190 88	0.175 52
FP	0.333 33	0.2764	0.236 82	0.2113	0.190 48	0.173 93	0.160 41

We summed up the short-time expansions [Eq. (1)] using the Levin series acceleration method [39,40]. Smith and Ford showed that the Levin method is very efficient in estimating sums of alternating sign power series, such as Eq. (1). In our case, the difference between the sixth and seventh Levin approximants is negligible and within the MC calculation error bars.

In Table II values of the $\rho_r(d)$ jamming densities are presented as a function of the dimensionality d . These values are computed using asymptotic expression [Eq. (7)], the MC values, the Levin summations using six coefficients, and the Fan-Percus (FP) [Eq. (8)] asymptotic expressions.

It is worth mentioning that for $d = 2$ the jamming density is known to a very high accuracy $\rho_r(d = 2) = 0.364\ 133\ 0(1)$ [27,36]. The asymptotic limit is an upper bound for all d . The convergence to its value is very fast. For $d = 4$, for instance, the asymptotic value is only higher by 4% than the MC result, and by less than 1% for $d = 8$. On the other hand, the FP high d approximation bounds the jamming densities from below, and it deviates from the MC value by 10% for $d = 4$, and by 9% for $d = 8$.

A numerical correction of the asymptotic limit ρ_{asy} [Eq. (9)] to fit the MC values for $2 \leq d \leq 8$, results in the expression

$$\rho_r(d) = \rho_{asy}(d) - 0.86\rho_{asy}(d)^{3.41} = \frac{\ln(1 + 2d)}{2d} \left[1 - 0.86 \left(\frac{\ln(1 + 2d)}{2d} \right)^{2.41} \right]. \quad (15)$$

The uncertainties (standard deviation errors) in the fitting parameters are 0.07 for the exponent and 0.06 for the coefficient. The deviation of the fit values from the MC calculated densities is at most 0.2%. In Fig. 3 the $\rho_{asy}(d)$, MC values, and the fitted value are presented versus d .

IV. RSA JAMMING DENSITIES OF d -DIMENSIONAL HYPERCUBES ON LATTICES (N_2 MODEL)

In this section we study the convergence rate of the jamming densities of the N_2 model to their asymptotic high d limit. In addition, we study the validity of the generalized Palasti approximation.

In 1960 Palasti [41] conjectured that the RSA jamming density of a system of parallel hard squares (also known as aligned squares) adsorbing on a continuum 2D surface, exactly equals the square of $\rho_{r,seg}$ —the jamming density of segments on a 1D line (car parking model),

$$\rho_{r,squares} = \rho_{r,seg}^2 = (0.747\ 597\ 9\dots)^2 = 0.558\ 902\ 6\dots \quad (16)$$

It has been shown by precise MC simulations [28] that the jamming density of the 2D parallel squares equals 0.562 009(4), 0.5% bigger than the Palasti value. Bonnier [42], using heuristic arguments, argued that although the conjecture is wrong, it is a good approximation for parallel hard hypercubes for all dimensions, i.e.,

$$\rho_r(d) \approx \rho_r(d = 1)^d. \quad (17)$$

The generalized Palasti approximation is an accurate approximation for the lattice analogues of the continuum models for $d = 2, 3$. For $d = 2$ the jamming density is bigger by 0.04% than the square of the 1D jamming density [27,43]. For $d = 3$ the jamming density is smaller by 0.2% from the Palasti value [33]. According to the generalized Palasti approximation, the jamming density decreases as a function of d as

$$\rho_r(d) \approx \rho_{Pal} = \left[\frac{1 - e^{-2}}{2} \right]^d = (0.432\ 332\dots)^d. \quad (18)$$

Note that here the density is defined as the ratio between the number of occupied sites (particles) to the total number L^d of lattice sites. In some other works (e.g., Refs. [33,43]) the density is defined as the ratio between the area (volume) of the adsorbed square (cubic) shells to the total area (volume). The latter density values are bigger by a factor of 2^d from the values here. In present units, the MC jamming density [43] of squares is $\rho_r(d = 2) = 0.186\ 985(1)$, and the MC jamming

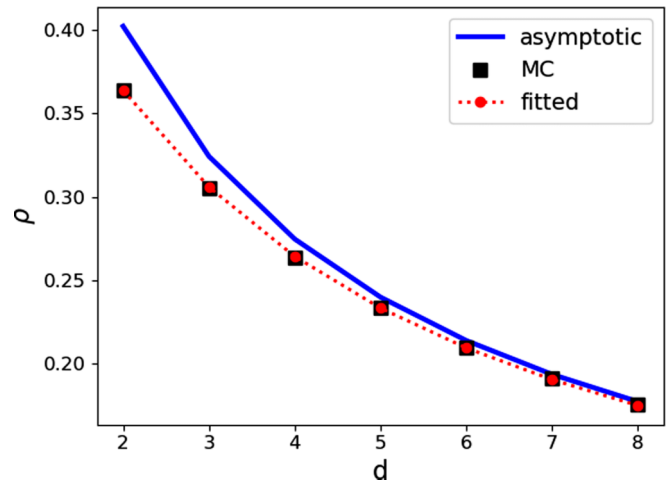


FIG. 3. $\rho_{asy}(d)$, MC values, and the fitted value [Eq. (15)] for a range of dimensions. Error bars are smaller than the symbols.

TABLE III. Deviation of Eqs. (19) and (18) from the MC results.

d	2	3	4	5	6	7	8	9	10
ρ_r	0.186 97	0.080 67	0.0346	0.014 70	0.006 167	0.002 55	0.001 035	0.000 412	0.000 16
MC/ ρ_{asy}	0.6807	0.6364	0.629 87	0.6476	0.681 18	0.7249	0.7729	0.8215	0.8739
MC/ ρ_{Pal}	1.0003	0.9983	0.9904	0.9733	0.9444	0.9033	0.8603	0.7808	0.7101

density of cubes is $\rho_r(d = 3) = 0.0806(1)$, where the number in parentheses is the uncertainty in the last digit.

The coordination number of a d -dimensional particle in the $N2$ model is $q = 3^d - 1$. As a result, the asymptotic high d jamming density is

$$\rho_{asy}(d) = \frac{d \ln(3)}{3^d - 1}, \tag{19}$$

substantially smaller than Eq. (18).

Since the interaction range of a $N2$ particle is greater than the unit length of the lattice, the probability to curl and form a compact lattice animal is not negligible, at least for $d = 2-4$. The resulting trees are expected to dominate for higher spatial dimensionalities. Therefore we extended the MC computations of the $N2$ model up to $d = 10$. The RSA filling algorithm is the same as for the $N1$ model. In Table III are presented the MC results, the ratio of the MC results to the asymptotic limit [Eq. (19)], and the ratio of the MC results to the Palasti approximations [Eq. (18)], as a function of d .

The jamming densities $\rho_r(d)$ converge very slowly to their asymptotic high d limit. The ratio increases monotonically only for $d > 4$. On the other hand, the Palasti approximation is an excellent approximation for $d = 2-5$, but it is an overshoot for higher values of d .

The coefficients $a_n(d)$ of the $N2$ model are extremely large numbers for $d > 3$, and their enumeration requires a lot of computation resources. Therefore we did not use them in the $\rho_r(d)$ estimation. In this case, in contrast to the $N1$ model, we did not find any formal correction relation between the $a_n(d)$'s and their high d limit.

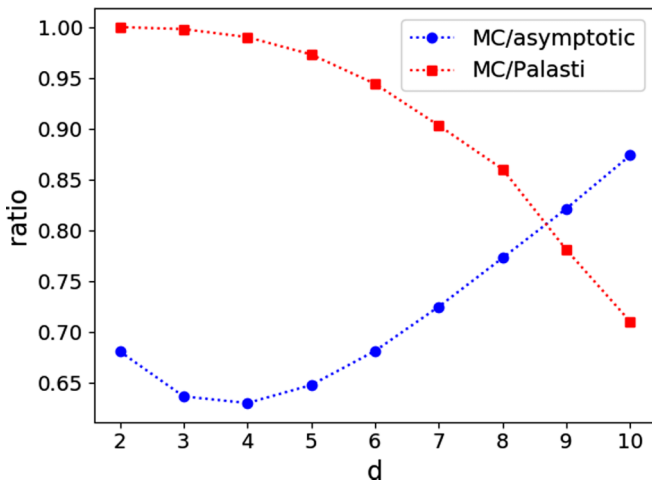


FIG. 4. d dependence of the ratio between MC results and the other estimations.

In Fig. 4 the ratios $\rho_r(\text{MC})/\rho_r(\text{asy})$ and $\rho_r(\text{MC})/\rho_r(\text{Palasti})$ are presented versus d .

V. SUMMARY

The high d approximation (tree graph approximation) to the dynamics of the RSA process depends only on the coordination number q of the repulsive interaction. For a given spatial dimensionality d , the accuracy of the high d approximation inversely depends on the range of the interaction.

For the $N1$ RSA process on the d -dimensional cubic lattice with a nearest-neighbor exclusion, the interaction range equals the lattice spacing and $q = 2d$. In this case, the high d approximation provides a very accurate approximation for the limiting jamming densities even for relatively low d values. For $d = 4$, for instance, the asymptotic result differs only by 4% from the “exact” MC result. For all $2 \leq d \leq 8$ the high d approximation appears to be an upper bound to the jamming densities $\rho_r(d)$. This observation requires more examination which is beyond the scope of the present work. The convergence rate of the approximation to the exact jamming densities as a function of d , vanishes as $[\frac{\ln(1+2d)}{2d}]^{3.41}$.

For all d and $n \leq 6$ the coefficients $a_n(d)$ of the short-time expansion [Eq. (1)] are given in terms of a correction finite sum of order $(n - 2)$ in $1/d$ to their asymptotic values [Eq. (5)]. It seems that this behavior is valid for all n , indicating that a closed-form expression may exist for all the coefficients (number of connected lattice animals) of the $N1$ model on the d -dimensional cubic lattice.

The high d tree approximation is less efficient for the $N2$ RSA process of d -dimensional hypercubes of length $k = 2$ on the hypercubic lattice. For $2 \leq d \leq 4$ the generalized Palasti approximation provides an excellent approximation to the jamming densities. For higher d values the decay of the jamming densities is substantially faster than the Palasti approximation [Eq. (18)], and it converges to the limit $\frac{d \ln(3)}{3^d}$ predicted by the high d approximation.

The interaction range of the $N1$ model equals the lattice spacing of the hypercubic lattice. Most of the empty neighbors of an occupied site extend out of the existing shell. As a result, the probability to curl inside and form a compact lattice animal is small even for relatively small d . On the other hand, the interaction range of a $N2$ particle is greater than the unit length of the lattice, and as a result an occupied site may have many nonvacant neighbors in the existing shell. Therefore, the probability to form a compact lattice animal is not negligible for $d = 2-4$. Trees start to dominate for higher values of d . As a result, the convergence of the jamming densities of the $N2$ model to their asymptotic high d values is slower than the convergence rate of the $N1$ jamming densities.

- [1] J. W. Evans, *Rev. Mod. Phys.* **65**, 1281 (1993).
- [2] M. C. Bartelet and V. Privman, *Int. J. Mod. Phys. B* **5**, 2883 (1991).
- [3] P. J. Flory, *J. Am. Chem. Soc.* **61**, 1518 (1939).
- [4] A. Rényi, *Publ. Math. Inst. Hung. Acad. Sci.* **3**, 109 (1958).
- [5] J. Feder, *Theo. Biol.* **87**, 237 (1980).
- [6] L. Finegold and J. T. Donnel, *Nature (London)* **278**, 443 (1979).
- [7] G. Y. Onoda and E. G. Liniger, *Phys. Rev. A* **33**, 715 (1986).
- [8] J. J. Ramsden, *J. Stat. Phys.* **73**, 853 (1993).
- [9] G. Fiumara and P. V. Giaquinta, *J. Phys. A* **27**, 4351 (1994).
- [10] E. Eisenberg and A. Baram, *Europhys. Lett.* **44**, 168 (1998).
- [11] E. Eisenberg and A. Baram, *J. Phys. A* **33**, 1729 (2000).
- [12] G. Parisi and F. Zamponi, *Rev. Mod. Phys.* **82**, 789 (2010).
- [13] P. M. Pasinetti, L. S. Ramirez, P. M. Centres, A. J. Ramirez-Pastor, and G. A. Cwilich, *Phys. Rev. E* **100**, 052114 (2019).
- [14] M. Cieřła and J. Barbasz, *J. Chem. Phys.* **137**, 044706 (2012).
- [15] J. H. Conway and N. J. A. Sloane, *Sphere Packings, Lattices and Groups* (Springer, New York, 1993).
- [16] H. L. Frisch and J. K. Percus, *Phys. Rev. E* **60**, 2942 (1999).
- [17] G. Parisi and F. Slanina, *Phys. Rev. E* **62**, 6554 (2000).
- [18] J. J. Gonzales, P. C. Hemmer, and J. S. Hoye, *Chem. Phys.* **3**, 228 (1973).
- [19] F. B. Pedersen and P. C. Hemmer, *J. Chem. Phys.* **98**, 2279 (1993).
- [20] Y. Fan and J. K. Percus, *J. Stat. Phys.* **66**, 263 (1992).
- [21] A. Baram and D. Kutasov, *J. Phys. A* **25**, L493 (1992).
- [22] A. Baram and A. Lipshtat, *Physica A* **561**, 125281 (2021).
- [23] A. Baram and D. Kutasov, *J. Phys. A* **22**, L855 (1989).
- [24] Y. Fan and J. K. Percus, *Phys. Rev. A* **44**, 5099 (1991).
- [25] Y. Pomeau, *J. Phys. A* **13**, L193 (1980).
- [26] R. H. Swendsen, *Phys. Rev. A* **24**, 504 (1981).
- [27] A. Baram and M. Fixman, *J. Chem. Phys.* **103**, 1929 (1995).
- [28] B. J. Brosilow, R. M. Ziff, and R. D. Vigil, *Phys. Rev. A* **43**, 631 (1991).
- [29] V. Privman, J.-S. Wang, and P. Nielaba, *Phys. Rev. B* **43**, 3366 (1991).
- [30] S. Torquato, O. U. Uche, and F. H. Stillinger, *Phys. Rev. E* **74**, 061308 (2006).
- [31] M. Cieřła, G. Pajak and R. M. Ziff, *J. Chem. Phys.* **145**, 044708 (2016).
- [32] G. Zhang, *Phys. Rev. E* **97**, 043311 (2018).
- [33] A. C. Buchini Labayen, P. M. Centres, P. M. Pasinetti, and A. J. Ramirez-Pastor, *Phys. Rev. E* **100**, 022136 (2019).
- [34] B. Widom, *J. Chem. Phys.* **58**, 4043 (1973).
- [35] R. Dickman, J. S. Wang, and I. Jensen, *J. Chem. Phys.* **94**, 8252 (1991).
- [36] C. K. Gan and J. S. Wang, *J. Chem. Phys.* **108**, 3010 (1998).
- [37] J. S. Wang, *Coll. Surf. A* **165**, 325 (2000).
- [38] M. Abramowitz and I. A. Stegun, *Handbook of Mathematical Functions* (Dover, New York, 1968), p. 824.
- [39] D. Levin, *Int. J. Comput. Math.* **3**, 371 (1973).
- [40] D. A. Smith and W. F. Ford, *SIAM J. Num. Anal.* **16**, 223 (1979).
- [41] I. Palásti, *Publ. Math. Inst. Hung. Acad. Sci.* **5**, 353 (1960).
- [42] B. Bonnier, *J. Phys. A* **34**, 10757 (2001).
- [43] A. J. Ramirez-Pastor, P. M. Centres, E. E. Vogel, and J. F. Valdes, *Phys. Rev. E* **99**, 042131 (2019).